The next time we used a platinum sample container and increased the pressure and temperature slightly. The result was practically one hundred percent coesite. We conducted further experiments within the pressure and temperature limits of 1800 – 2000 °C. We again obtained coesite, but there was an essential difference. An unknown phase with a high refractive index and high birefringence appeared systematically. It either bordered the coesite or formed flaky and needle-shaped grains. I designated this phase in the notebook as phase X. Phase X always appeared as an admixture — perhaps because there had not been time for a complete transformation? We decided to hold the next sample of quartz under these conditions for three hours. The result was an explosion. Another lengthy test — again an explosion. It was necessary to make water jackets to cool the external parts of the high-pressure chamber. And thus, the first test with the jackets. As before the pressure was higher than the last transition point in bismuth. The temperature was approximately 2000 °. I maintained these conditions for two hours. Everything was in order; the chamber did not break. I extracted the platinum container. I noticed a certain difference. If before it had been enough to tear off the lid of the container for the contents to pour out easily and the walls of the container to appear clean, this time part of the contents adhered to the lid. I took the material from the center of the container. It was practically pure coesite. I noticed phase X. There was somewhat more than before. In the course of a week I mounted a second and third test. The results were the same. As before I ignored the material adhering to the lid.

I performed a test at lower temperature. I extracted the container. What was this? The lid was impossible to remove. I tried to tear it from the side surface of the container, without success. Finally I removed the lid with pliers, extracted some of the substance and put it under the microscope. There was neither quartz nor coesite. An unknown fibrous material with a high refractive index. Yes, this was phase X, difficult to recognize when there was so much of it. There were some individual needle-shaped formations and even well-formed long crystals. Some of the crystals appeared to be green in the cross Nicol prisms. I started to guess confusedly what had happened: we had put on cooling jackets with flowing water, the thermal conductivity was increased, the temperature in the chamber had decreased, and we appeared to be in the stability field of the new phase.

Then it was a matter of analytical chemistry. By the way, it was still necessary to prove that all this was a new phase. I was quite worried by the possibility of contamination of the silica with carbon, that some carbon compounds could be formed, etc. Finally after numerous checkings and examinations, discussions and hesitations we appeared to be quite sure that a new dense phase of silica had been discovered. A paper was written and submitted for publication. I am omitting plenty of complications that are of no interest.

In August of 1961, the paper was published and received much attention. And then, in December 1961, I received a letter from Edward Chao, in which he reported the discovery of a new mineral, a natural analog of the phase X, at Meteor Crater in Arizona. Chao also wrote that the new phase was named stishovite.

The scientific part of the discovery story ended with those events. What followed was quite a different story.

PACS number: 81.30.Hd
DOI: 10.1070/PU2002v045n04ABEH001155

Stishovite and its implications in geophysics: new results from shock-wave experiments and theoretical modeling

S-N Luo, J L Mosenfelder, P D Asimow, T J Ahrens

1. Introduction

Pure stishovite and coesite samples with densities of 4.31 ± 0.04 and 2.92 ± 0.03 g cm^{-3}, respectively, and dimensions appropriate for planar shock-wave experiments have been synthesized with a multi-anvil high-pressure press. The principal Hugoniot centered at stishovite obtained by shock loading up to 235 GPa yields a linear shock velocity (U_s) – particle velocity (u_p) relationship $U_s = C_0 + su_p$, where $C_0 = 9.08$ km s^{-1}, and $s = 1.23$. The new shock-wave data for coesite to 140 GPa agree with, and extend, the former study. These data along with previous studies on other polymorphs now provide Hugoniots for the major polymorphs of SiO_2 (fused quartz, quartz, coesite and stishovite). The Grüneisen parameter for stishovite under compression obtained from the internal energy and pressure differences between different principal Hugoniots of silica polymorphs is $\gamma = 1.35(V/V_0)^q$, where $q = 2.6 \pm 0.2$. Previously melting of stishovite at 70 and 113 GPa was inferred from shock temperature measurements. These are in accord with recent molecular dynamics modeling of the high-pressure fusion curve of stishovite.

Silica is important not only as the main constituent of the Earth and other terrestrial planets but also as a model system to study the fundamental physics of material properties, such as polymorphic phase changes and interatomic potentials [1]. To understand the seismic structure of the Earth and transport processes (e.g., heat and mass), knowledge of thermodynamics of the $MgO - SiO_2$ system is crucial. Free silica may exist as stishovite (or post-stishovite phases) in the Earth from 300 km depth (10 GPa) in the upper mantle to 2891 km at the core-mantle boundary (CMB, 136 GPa). Stishovite-type phases may play a key role in chemical reactions in the lowermost mantle [1 – 3]:

$$(Mg_{0.9}Fe_{0.1})\,SiO_3\,(\text{perovskite}) + 0.15Fe(\text{liquid}) \leftrightarrow 0.9MgSiO_3(\text{perovskite}) + 0.2FeO(\text{hpp}) + 0.05FeSi(\text{liquid}) + 0.05SiO_2(\text{stishovite})\,, \quad (1)$$

$$(Mg,\ Fe)O(B1) + SiO_2(\text{stishovite}) \leftrightarrow (Mg, Fe)SiO_3(\text{perovskite}). \quad (2)$$

These reactions sequester iron from the mantle into the metallic core and consume silica into Mg-perovskite and may have occurred during the early accretion history of the Earth [3]. In this sense free silica might be scarce at the lower mantle. Stishovite was the first silicate discovered with Si^{4+} octahedral coordination with O^{2-}, characteristic of all the lower mantle silicate phases, and the elastic, thermodynamic and transport properties of stishovite in joint presence with other materials remain important for seismic and geodynamic studies of the Earth. Stishovite and post-stishovite phases are also important for planetary impact processes: the structure

of shocked SiO_2-bearing rocks and meteorites constrains the interpretation of impact process [4, 5].

Extensive and detailed studies on the silica system have been conducted for a long time with various techniques [1]. For shock wave experiments, McQueen et al. [6] reanalyzed the first shock-wave studies on fused quartz and quartz by Wackerle [7] and demonstrated that the high-pressure region above 30 GPa for both initially crystal quartz and fused quartz appeared to behave as if transition to the recently discovered rutile phase had occurred. They predicted $C_0 = 10.0$ km s^{-1} and $s = 1.0$ for the stishovite Hugoniot. Additional studies such as those by Fowles [8], Ahrens and Rosenberg [9] and some Russian studies (see Trunin [10] and references cited therein for a complete review) on crystal and porous quartz, fused silica, crystobalite and coesite all demonstrated the transition to stishovite as suggested by McQueen et al. [6]. Podurets et al. [11] proposed the stishovite Hugoniot as $C_0 = 7.6$ km s^{-1} and $s = 1.41$, based on their shock-wave experiments. Furnish and Ito [12] had synthesized polycrystalline stishovite for shock-wave measurements. Unfortunately, their samples were heterogeneous. They varied in both porosity and stishovite content such that the initial bulk densities varied from 3.8 to 4.07 g cm^{-3}. This gave rise to a considerable scatter in the resulting data. Although the shock-compressed states are undeniably compressed stishovite, the data are too scattered to provide an independent contribution to our knowledge of the equation of state of this phase. Direct measurement of the Hugoniot of stishovite is of paramount importance as suggested by Trunin [10].

Advances in static synthesis techniques, shock-wave diagnostics and theoretical modeling enable further study of high-pressure silica phases [13, 14]. To address the equation of state and the post-stishovite transition along the Hugoniot [10], direct shock-wave loading of stishovite is realized by the synthesis of pure stishovite samples with dimensions circumventing edge effects and ensuring high accuracy of measurement in planar impact experiments [13]. The melting point of stishovite at 70 and 113 GPa was previously inferred from shock-induced melting experiments [15]. New molecular dynamics modeling of stishovite melting [14] complements the shock-wave study. In this review, we summarize our experimental work on high-pressure phases of silica and theoretical study of the phase diagram of stishovite.

2. Static synthesis and dynamic loading of coesite and stishovite

To conduct planar shock-wave loading on a light gas gun, the diameter to thickness ratio of the sample should be larger than 3 to avoid edge effects. The accuracy of the present shock-wave velocity measurement (± 1 ns) is limited by the streak camera capable of measuring 80 – 100 ns propagation time in a 1 mm thick stishovite or coesite sample. This presents a challenge for the synthesis of stishovite with multi-anvil high-pressure press: the minimum required dimensions are 3 mm in diameter and 1 mm in thickness. Previously typical dimensions of the recovered sample in laboratory the multi-anvil cells that reach 10 GPa are ~ 1.5 mm in diameter [16]. A new technique was adopted to radically simplify the assembly to maximize space, at the expense of exact characterization of the sample environment [13]. In the synthesis experiments, success is justified by the recovered phase, and precise pressure (P) and temperature (T) control is not important. For this reason, the ZrO_2 insulator, $LaCrO_3$ heater, MgO spacer, and Pt capsule typically used in modern multi-anvil experiments [16] were dispensed with and only a Re foil was used as both heating element and sample container. The stishovite samples were synthesized using 14-mm sintered MgO octahedra, 8-mm truncation-edge-length carbide anvils and pyrophyllite gaskets. The temperature is monitored with a W/Re thermocouple, and the pressure is calculated from the loading calibration. The starting material is a cylinder of pure silica glass. Stishovite samples have been synthesized at 14 GPa and 1000 °C, with a bulk density of (4.31 ± 0.04) g cm^{-3}, diameter of about 4 mm, and thickness of about 2.5 mm. The density was measured using the Archimedean method with toluene as the immersion liquid, and quartz as a calibration standard. These samples are pure stishovite with zero porosity as evidenced by optical microscopy and X-ray diffraction (XRD) patterns [13].

Coesite samples have been synthesized with the cubic module in the multi-anvil press at approximately 4 GPa and 900 °C. The pressure medium is a 21-mm pyrophyllite cube with a barium carbonate sleeve surrounding the graphite heater. The square anvil truncations are 16 mm along each edge. The starting material is silica glass. The final products have bulk densities of (2.92 ± 0.03) g cm^{-3} and XRD patterns with only coesite peaks. The coesite samples are ~ 5.3 mm in diameter, and ~ 5 mm in length.

The synthesized coesite and stishovite samples are sectioned into disks and polished for shock-wave experiments. The stishovite and coesite samples mounted in the target assembly have diameter/thickness ratios of approximately 4 and 5, respectively. Coesite and stishovite samples were mounted in the same target assembly when possible. Planar impact experiments have been conducted on the Caltech two-stage light gas gun with a streak camera measuring the shock velocity, and flash X-ray diagnostics the projectile velocity [13]. By varying the flyer – driver material and projectile velocity, different final states were achieved in the shocked coesite and stishovite samples. The directly measured projectile velocity and shock velocity (U_s) were reduced to shock-state particle velocity (u_p), pressure (P) and specific volume (V) in the sample by the impedance match method [17]. Figure 1 shows the $U_s - u_p$ relationships for stishovite and coesite. The new coesite data are in agreement with Podurets et al. [11] A linear fit to both coesite data sets in stishovite regime gives

$$U_s \ (\text{km s}^{-1}) = 2.52 + 1.70\,u_p; \quad \rho_0 = (2.92 \pm 0.03) \ \text{g cm}^{-3}. \tag{3}$$

A linear fit to the stishovite data yields

$$U_s \ (\text{km s}^{-1}) = 9.08 + 1.23\,u_p; \quad \rho_0 = (4.31 \pm 0.04) \ \text{g cm}^{-3}. \tag{4}$$

The corresponding Hugoniot in the $P-V$ plane for stishovite is shown in Fig. 2 along with the diamond-anvil cell (DAC) data at low pressures. The stishovite fit to the Vinet universal equation of state [18] yields $K_0 = (326 \pm 4)$ GPa and $K_0' = 4.8 \pm 0.2$, comparable to $K_0 = (298 \pm 8)$ GPa and $K_0' = 3.98 \pm 0.46$ at 300 K by Hemley et al. [1]. The Vinet fit is essentially the same as the curve mapped from the $U_s - u_p$ fit. The comparison between the stishovite Hugoniot and DAC results (300 K isotherm) shows that the Hugoniot lies slightly above but very close to the 300 K isotherm at pressures up to

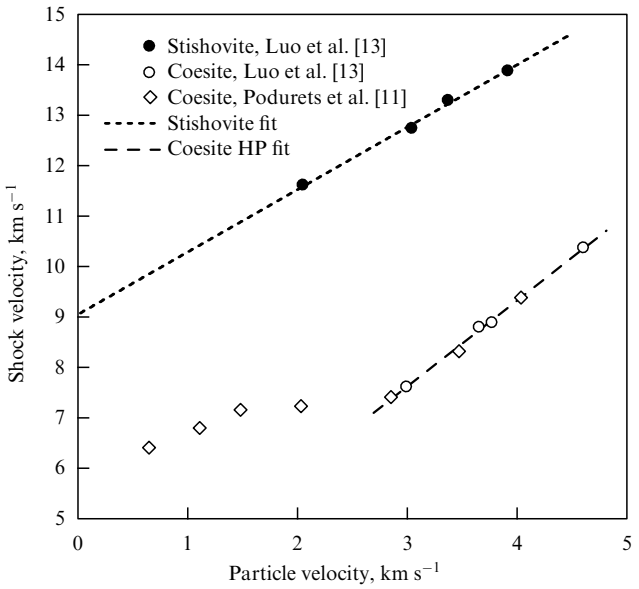

Figure 1. $U_s - u_p$ relationships for stishovite and coesite [11, 13]. Stishovite: U_s (km s^{-1}) $= 9.08 + 1.23\,u_p$, $\rho_0 = (4.31 \pm 0.04)$ g cm^{-3}. Coesite in high-pressure regime (HP): U_s (km s^{-1}) $= 2.52 + 1.70\,u_p$, $\rho_0 = (2.92 \pm 0.03)$ g cm^{-3}.

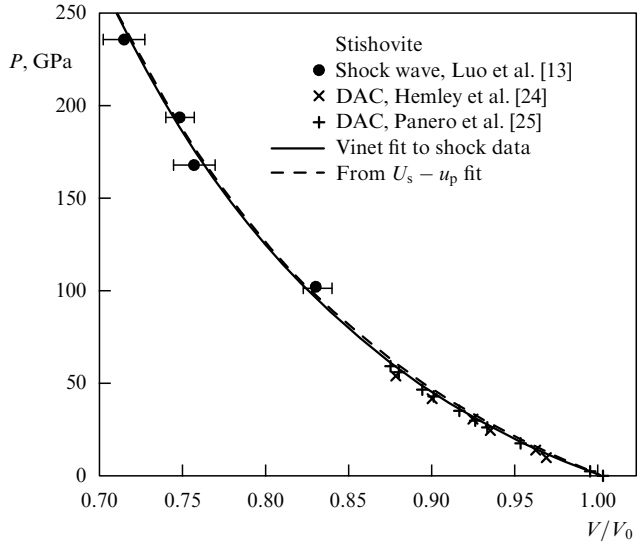

Figure 2. Stishovite $P-V$ Hugoniot [13] with diamond-anvil cell (DAC) data [24, 25]. V_0 is the ambient specific volume of stishovite.

55 GPa, suggesting that the Hugoniot is relatively cold (a rough estimation shows that the temperature at Hugoniot is about 1600 K at 260 GPa). This is consistent with the small compressibility of stishovite. On the contrary, shocked fused quartz is melted at 4500 K and 70 GPa, and α-quartz at 4750 K and 113 GPa as demonstrated by shock temperature measurements [15]. Evidence for post-stishovite phases is not pronounced in the stishovite principal Hugoniot. One possible reason is that the transition is kinetically impeded, although the possibility exists that the minor structural changes of stishovite to post-stishovite cannot be resolved from Hugoniots in $U_s - u_p$ and $P - V$ space. It was proposed that the transition to post-stishovite is exhibited in the fused quartz and quartz principal Hugoniots [19] but it is not evident in the stishovite principal Hugoniot. This could be due to the different shock temperatures along Hugoniots for different silica polymorphs.

Principal Hugoniots centered at four different silica polymorphs have now been obtained. Figure 3 shows the principal Hugoniots for quartz, coesite and stishovite. The fused quartz data are badly scattered and not included. At high pressure, where all the three Hugoniots are in the stishovite phase, the internal energy and pressure differences at fixed volume allow estimation of the Grüneisen parameter (γ) of stishovite by finite difference. The Hugoniots in the stishovite regime for quartz and coesite are obtained by fitting to the available data. The Grüneisen parameter for stishovite, $\gamma(V)$, is obtained (see Fig. 4) from quartz–stishovite and coesite–stishovite Hugoniot pairs. The fitting to

$$\gamma = \gamma_0 (V/V_0)^q, \quad \text{with} \quad \gamma_0 = 1.35, \tag{5}$$

yields $q = 2.6 \pm 0.2$. The $\gamma(V)$ obtained from the quartz–stishovite pair is slightly different from that from the coesite–stishovite pair. This could be due to the temperature dependence of γ. The Grüneisen parameter for stishovite at high pressure obtained directly from shock-wave experiments provides an important constraint on thermodynamic calculations.

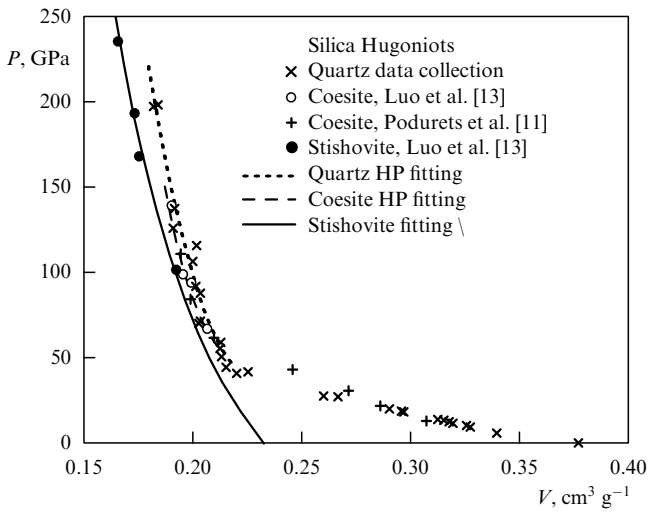

Figure 3. $P-V$ Hugoniots for quartz [7, 26, 27], coesite [11, 13] and stishovite [13].

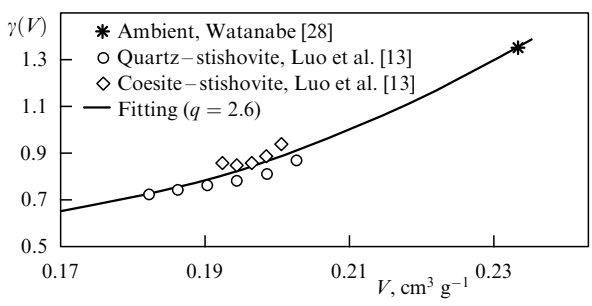

Figure 4. Grüneisen parameter $\gamma(V)$ for stishovite obtained from the $P-V$ Hugoniots of quartz, coesite and stishovite using the Mie–Grüneisen equation of state [13, 28].

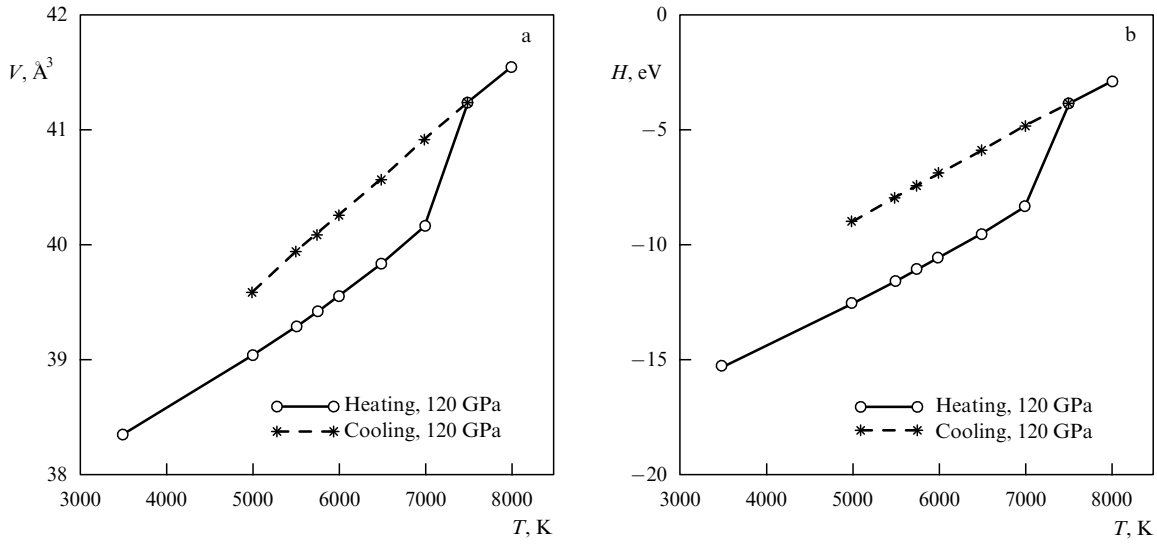

Figure 5. Single-phase simulation of stishovite melting at 120 GPa with molecular dynamics [14]. (a) The unit cell (2 SiO_2 formulae) volume, and (b) the corresponding enthalpy during the heating – cooling process.

3. Melting curve of stishovite

Stishovite melting at high pressure has been investigated by using techniques such as shock temperature measurements [15] and the diamond-anvil cell experiment [20]. It is still challenging to determine the phase diagram from dynamic and static experiments at high pressures. Several theoretical studies have tackled this issue [14, 21]. The new molecular dynamics (MD) simulations [14] employing Morse – stretch charge equilibrium potential (MS – Q) yielded results in agreement with the shock melting and DAC experiments. In the MD stishovite melting simulation, single- and two-phase simulation methods were utilized. Figure 5 shows an example of the single-phase simulation at 120 GPa. The transition temperature (7000 K) from solid to liquid stishovite is the melting point (T_m) at 120 GPa from the single-phase simulation. The slope of the melting curve (dT_m/dP) can be determined from volume and enthalpy changes using the Clausius – Clapeyron equation. One

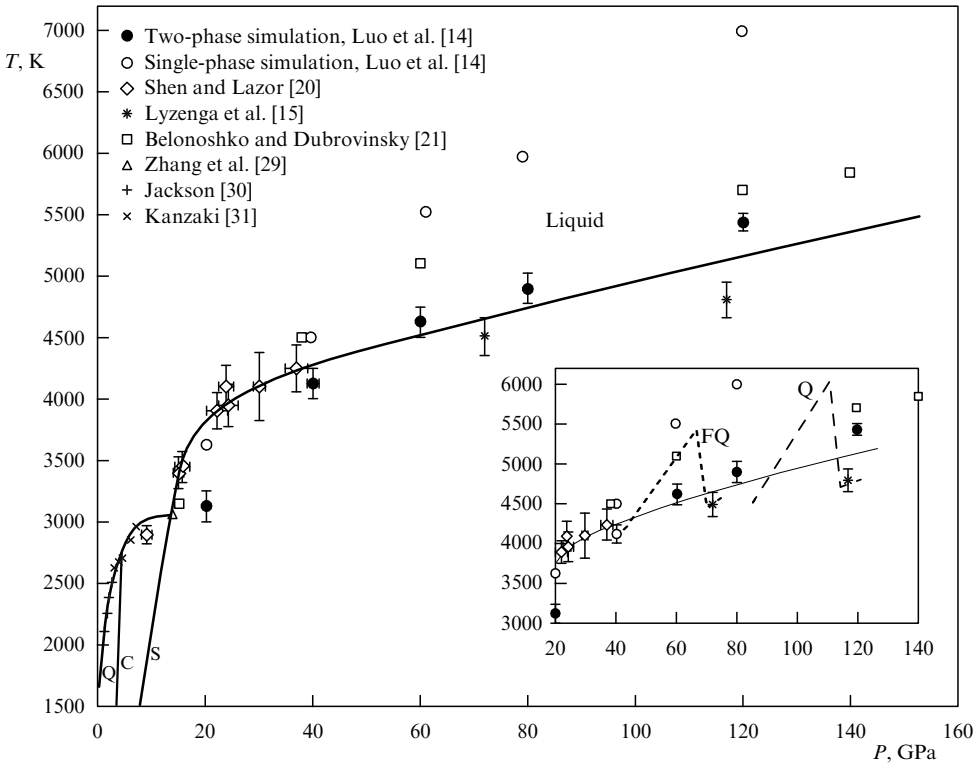

Figure 6. Melting curve of stishovite and silica phase diagram from theoretical and experimental studies [14, 15, 20, 21, 29 – 31]. The solid lines are phase boundaries: Q — quartz; C — coesite; S — stishovite, and FQ — fused quartz. (inset) Dashed lines are the shock temperature measurement of shocked fused quartz and quartz [15]. The sharp drop of temperature indicates the melting of stishovite. The portions of Hugoniots above the melting curve (solid line) represent superheated stishovite solid in the shock states.

problem with single-phase melting simulations is the possible superheating of the solid during heating and undercooling of the liquid during cooling due to the kinetics [22] especially at high pressure, which could be reduced by two-phase simulation [23]. The two-phase simulation was conducted by constructing a solid–liquid model by combining the solid and liquid models at the same pressure and temperature from the single-phase simulation. Figure 6 shows the simulation results along with former studies on stishovite melting. At 20 GPa, single-phase simulation appears to be closer to experimental data than the two-phase simulation, possibly due to the simplicity of the force field or the interface effect that is more pronounced at low pressure [14]. At high pressures, the two-phase simulation yielded more accurate results. The melting curve of stishovite is obtained from MD simulation results along with experimental data. The slope of the proposed melting curve is consistent with that computed from single-phase simulation. The MD simulation results are close to the static DAC results at low pressure, and shock wave data at high pressure. This appears to validate the interpretation of superheating of the solid along fused quartz and quartz Hugoniots by Lyzenga et al. [15]. With the melting curve of stishovite constrained, the silica phase diagram is extended to the megabar regime.

4. Conclusion

In conclusion, the Hugoniot of stishovite up to 235 GPa was obtained by shocking pure stishovite samples synthesized from a multi-anvil high-pressure press. The coesite Hugoniot in the stishovite regime is in agreement with former study and extended to 140 GPa. Hugoniots centered at various silica polymorphs have been obtained, from which the Grüneisen parameter for stishovite under compression is experimentally determined. The new molecular dynamics modeling validates the interpretation of shock melting experiments on fused quartz and quartz, and the phase diagram of silica is extended to the megabar regime with a sound experimental and theoretical basis.

Acknowledgment. Contribution No. 8856, Division of Geological and Planetary Sciences, California Institute of Technology.

References

1. Hemley R J, Prewitt C T, Kingma K *Rev. Mineral.* **29** 41 (1994)
2. Knittle E, Jeanloz R *Science* **251** 1438 (1991)
3. Song X, Ahrens T J *Geophys. Res. Lett.* **21** 153 (1994)
4. Chao E C T et al. *J. Geophys. Res.* **67** 419 (1962)
5. El Goresy A et al. *Science* **288** 1632 (2000)
6. McQueen R G, Fritz J N, Marsh S P *J. Geophys. Res.* **68** 2319 (1963)
7. Wackerle J *J. Appl. Phys.* **33** 922 (1962)
8. Fowles R *J. Geophys. Res.* **72** 5729 (1970)
9. Ahrens T J, Rosenberg J T, in *Shock Metamorphism of Natural Materials* (Eds B M French, N M Short) (Baltimore: Mono Book Corp., 1968) p. 59
10. Trunin R F *Shock Compression of Condensed Materials* (Cambridge: Cambridge Univ. Press, 1998)
11. Podurets M A et al. *Izv. Akad. Nauk SSSR Fiz. Zemli* **17** 9 (1981)
12. Ito E, Furnish M D, Sandia Report SAND-95-2342 (1995)
13. Luo S-N et al. *Geophys. Res. Lett.* (2002), in press
14. Luo S-N et al. *Earth Planet. Sci. Lett.* (2002), in press
15. Lyzenga G A, Ahrens T J, Mitchell A C *J. Geophys. Res.* **88** 2431 (1983)
16. Rubie D C *Phase Transitions* **68** 431 (1999)
17. Ahrens T J, in *High Pressure Shock Compression of Solids* (Eds J R Asay, M Shahinpoor) (New York: Springer-Verlag, 1993) pp. 75–114
18. Cohen R E, Gülseren O, Hemley R J *Am. Mineral.* **85** 338 (2000)
19. Akins J (Private communication)
20. Shen G, Lazor P *J. Geophys. Res.* **100** 17699 (1995)
21. Belonoshko A B, Dubrovinsky L S *Geochim. Cosmochim. Acta* **59** 1883 (1995)
22. Allen M P, Tildesley D J *Computer Simulation of Liquids* (Oxford: Clarendon Press, 1987)
23. Strachan A, Çağin T, Goddard W A III *Phys. Rev. B* **60** 15084 (1999)
24. Hemley R J et al. *Solid State Commun.* **114** 527 (2000)
25. Panero W R, Benedetti L R, Jeanloz R *J. Geophys. Res.* (2001), submitted
26. Marsh S P *LASL Shock Hugoniot Data* (Berkeley: Univ. of California Press, 1980)
27. Al'tshuler L V, Trunin R F, Simakov G V *Izv. Akad. Nauk SSSR Fiz. Zemli* (10) 1 (1965)
28. Watanabe H, in *High-Pressure Research in Geophysics* (Adv. in Earth and Planetary Sci., Vol. 12, Eds S Akimoto, M H Manghnani) (Tokyo: Center for Acad. Publ. Japan, 1982) pp. 441–464
29. Zhang J et al. *J. Geophys. Res.* **98** 19785 (1993)
30. Jackson I *Phys. Earth Planet Int.* **13** 218 (1976)
31. Kanzaki M *J. Am. Ceram. Soc.* **3** 3706 (1990)

PACS numbers: 61.50.Ks, 91.35.Gf, 91.35.Lj

DOI: 10.1070/PU2002v045n04ABEH001159

Minerals of the deep geospheres

D Yu Pushcharovskiĭ

In this report I discuss the composition and structure of the Earth's mantle. Analysis of seismic tomography maps and the data on the material composition of the mantle shows that the mantle consists of several concentric zones, instead of the commonly accepted two zones, the upper and the lower. As in the Earth's crust, silicates are the predominant substance of the mantle, but structurally the silicates of the mantle differ substantially from those of the crust. More than one hundred tetrahedron complexes in the silicates of the Earth crust are replaced by no more than 20 structure types of this class of minerals in the mantle, and the main difference between these types lies in the transformation of Si tetrahedrons into Si octahedrons. In this sense, one can say that stishovite has opened up a new chapter of the crystal chemistry of silicates. New data on the structural transformations of minerals in the deep geospheres suggest that the mineralogical diversity of the deep zones of the mantle is much poorer than that of the Earth's crust, but nevertheless the mantle mineralogy is not as primitive as it was believed even two to three decades ago.

One of the most intriguing problems of geology in the past decades is related to studies of the composition and structure of the deep geospheres of the Earth. Such research in the Earth sciences is of top priority, since more than 90% of matter in the universe is under pressures greater than 1 GPa. The pressure range in the universe is enormous: pressures vary by more than 60 orders of magnitude. In intergalactic space, there is one atom to more than one cubic centimeter of space, while at the center of neutron stars the state of matter is comparable to the Sun's mass (which is approximately 300 thousand times greater than the Earth's mass) compacted into a volume smaller than that of the Earth (the Earth's volume is approximately one million times smaller than the Sun's).